INTERNATIONAL JOURNAL OF HYDROGEN ENERGY 43 (2018) 9599–9606

Available online at www.sciencedirect.com

ScienceDirect

journal homepage: www.elsevier.com/locate/he

Hydrogen production rates with closely-spaced felt anodes and cathodes compared to brush anodes in two-chamber microbial electrolysis cells

Emily Zikmund, Kyoung-Yeol Kim, Bruce E. Logan *

Department of Civil and Environmental Engineering, The Pennsylvania State University, 231Q Sackett Building, University Park, PA, 16802, USA

ARTICLE INFO

Article history:
Received 14 February 2018
Received in revised form
3 April 2018
Accepted 7 April 2018
Available online 26 April 2018

Keywords:
Felt anode
Brush anode
Hydrogen production
Two-chamber
Microbial electrolysis cell

ABSTRACT

Flat anodes placed close to the cathode or membrane to reduce distances between electrodes in microbial electrolysis cells (MECs) could be used to develop compact reactors, in contrast to microbial fuel cells (MFCs) where electrodes cannot be too close due to oxygen crossover from the cathode to the anode that reduces performance. Graphite fiber brush anodes are often used in MECs due to their proven performance in MFCs. However, brush anodes have not been directly compared to flat anodes in MECs, which are completely anaerobic, and therefore oxygen crossover is not a factor for felt or brush anodes. MEC performance was compared using flat felt or brush anodes in two-chamber, cubic type MECs operated in fed-batch mode, using acetate in a 50 mM phosphate buffer. Despite placement of felt anodes next to the membrane, MECs with felt anodes had a lower hydrogen gas production rate of 0.32 ± 0.02 m^3-H_2/m^3-d than brush anodes (0.38 ± 0.02 m^3-H_2/m^3-d). The main reason for the reduced performance was substrate-limited mass transfer to the felt anodes. To reduce mass transfer limitations, the felt anode electrolyte was stirred, which increased the hydrogen gas production rate to 0.41 ± 0.04 m^3-H_2/m^3-d. These results demonstrate brush electrodes can improve performance of bio-electrochemical reactors even under fully anaerobic conditions.

Introduction

Microbial electrolysis cells (MECs) are being investigated as a method of renewable hydrogen gas production using waste biomass [1–7]. Exoelectrogenic bacteria on the anode of an MEC use biodegradable organic matter, for example in wastewaters or fermentation effluents, as the fuel for current generation, with hydrogen gas produced electrochemically at the cathode [8,9]. The voltage produced by the bacteria is not sufficient to generate hydrogen gas at the cathode, and thus voltage must be added to the circuit to drive electrochemical hydrogen production [5,8,10]. MECs are therefore a green method for hydrogen gas production as long as the additional energy required for MEC operation is supplied by a renewable energy source such as solar, wind, salinity gradient energy, or by waste biomass powered microbial fuel cells (MFCs) [11,12]. Electrical power is generated in MFCs using the same type of anode and reactor structure as an MEC, with an exoelectrogenic biofilm on the anode, but oxygen is used as the final

* *Corresponding author.*
E-mail address: blogan@psu.edu (B.E. Logan).
https://doi.org/10.1016/j.ijhydene.2018.04.059
0360-3199/

electron acceptor at the cathode in an MFC producing a spontaneous reaction [13].

To maximize hydrogen gas production rates per volume of reactor in MECs, or current generation in MFCs, thin electrode chambers should be used in order to provide a high specific electrode surface area of the electrodes (area of electrodes per volume of reactor) [14–17]. Placing the electrodes close to each other not only produces a more compact reactor design, the close electrode spacing also reduces the internal resistance of the system by minimizing the solution resistance. However, when flat electrodes were used in MFCs with an electrode spacing of <2 cm, power was decreased despite the reduction in solution resistance, due to oxygen crossover from the cathode to the anode [18,19]. In the presence of dissolved oxygen, the anode potential becomes more positive which reduces the voltage and therefore power production. With cylindrical-shaped graphite fiber brush anodes, however, a more negative anode potential is maintained even when the brush is very close to the air-cathode (<0.5 cm), resulting in high power generation [20,21]. Thus, power densities in MFCs with brush anodes placed close to the cathode (1.36 ± 0.20 W/m^2 for studies in our laboratory at Penn State, or 1.11 ± 0.45 W/m^2 at many different locations [22]) are higher than those with flat carbon cloth or felt anodes (1.05 W/m^2 in our laboratory using carbon felt [23], compared to 0.79 ± 0.19 W/m^2 using carbon felt and 0.51 ± 0.00 W/m^2 using carbon cloth at different locations) [22]. The impact of flat anode size and electrode spacing has been extensively tested in MFCs [23–29] but not in MECs. In one study where the thickness of the anode was examined in an MEC with a cloth separator between the electrodes, the current increased by using a thicker anode, but net hydrogen gas production did not improve [24]. The main reason for a lack of improved hydrogen recovery was likely hydrogen gas crossover to the anode, as this can enhance current production but not increase hydrogen gas recovery (hydrogen gas is consumed by anodic bacteria or loss of hydrogen to methane production) [30–33]. While the use of an ion exchange membrane can reduce hydrogen losses [34,35], flat and brush anodes have not been compared in two chamber MECs with closely-spaced electrodes and an ion exchange membrane as the separator.

In this study, we compared the performance of flat felt anodes to commonly used brush anodes in MECs using typical fuel (acetate), electrolyte (50 mM phosphate buffer), and reactor conditions (3 cm diameter, cube shaped reactors) [22]. Both the felt and brush anodes were placed adjacent to the ion exchange membrane to minimize ohmic resistances. MEC performance was compared by measuring the current densities, total hydrogen production rates and chemical oxygen demand (COD) removals based on a complete fed-batch cycle, and energy recoveries relative to the electrical energy consumed by the systems.

Materials and methods

Anodes and their acclimation in MFCs

Two types of anodes were examined for performance in MFCs and MECs, cylinder-shaped graphite fiber brush anodes, and flat disc-shaped felt anodes. Brush anodes (2.5 cm length, 1.5 cm diameter, encased volume of 4.4 cm^3) were made from carbon fibers twisted between two titanium wires (PANEX 33 160K, ZOLTEK) [21,36]. Carbon felt anodes (0.64 cm thick, Alfa Aesar, Ward Hill, MA) were cut into circles with a 7 cm^2 cross sectional surface area (encased volume of 4.5 cm^3) [23]. Both types of anodes were acclimated for stable current generation in single chamber MFCs prior to their use in MECs. Brush anodes were placed across the middle of the 2 cm wide anode chamber (14 mL volume), so that the stem was parallel to the cathode reactor, with only a small gap (calculated to be 0.25 cm, but in effect only <0.3 cm based on variations in brush fiber lengths) between the brush outer surface and the cathode (Fig. S1a). While this configuration resulted in a brush that did not fully cover the cathode, which can lower power production relative to complete surface coverage [25,37], this placement enabled the use of a 2.5 cm long brush in a 2 cm wide chamber due to its 1.5 cm diameter. To minimize the impact of oxygen intrusion on felt anode acclimation in MFCs, the felt anodes were placed on the opposite side of the chamber from the cathode in 4 cm long reactors with a volume of 28 mL, instead of the 2 cm long chambers [37]. All anodes were heat treated for 30 min at 450 °C in a muffle furnace before being placed into the MFCs [36]. The cathodes for the MFCs were activated carbon cathodes produced by VITO (Mo, Belgium) [38–40].

MEC reactor configuration

Two chamber MECs were constructed that had 3 cm diameter chambers formed in cubes of polycarbonate, with 2 cm long anode chambers and 4 cm long cathode chambers (28 mL of liquid with 7 mL in headspace) (Fig. 1) [34]. The anode and cathode chambers were separated by an AEM (anion exchange membrane, Selemion AMV, AGC Engineering Co. Ltd., JP). The anode chambers for the brush anodes were the same as those used in the MFCs. The lengths of the anode chambers for the MFCs with felt anodes were changed to 2 cm. The felt anodes were removed from the MFCs and placed against the AEM, with a ring of titanium foil pressed against the felt to function as a current collector. The working volumes of the anode chambers were 16 mL for the brush anode (with minimal water displacement by the electrode), and 14 mL for the felt anode (2 mL water displacement). The smaller volume of water for the felt anode was due to the water displacement for the lower porosity felt anode, the volume displaced by the gasket to hold it in place, and the curvature (bowing out) of the felt that trapped some water between the felt and the membrane so that it was not replaced when the fluid in the MEC was changed (Fig. 1). For the brush anode MEC, the brush anode spanned a distance of 0.25–1.75 cm of the 2 cm thick chamber (although it did not fully cover the AEM), while the felt anode extended only 0.64 cm into the fluid but completely covered the AEM.

The cathodes for all reactors were discs of stainless steel mesh (7 cm^2) containing a platinum catalyst and carbon black (0.5 mg/cm^2, 10% Pt and Vulcan XC-72), with a Nafion binder (5 wt% solution, Aldrich Nafion® perfluorinated ion-exchange resin) as previously described [34]. Cathodes were placed 1 cm from the AEM to avoid trapping hydrogen gas between the

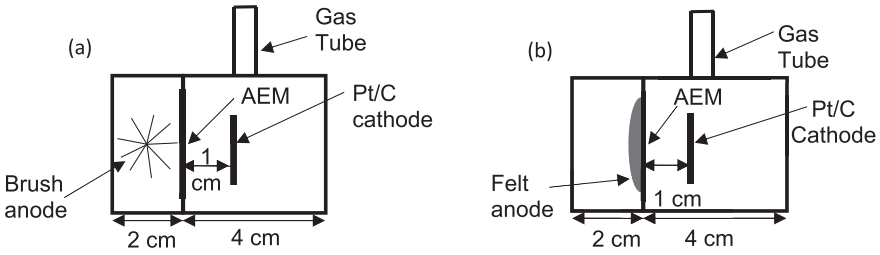

Fig. 1 – MEC configuration and anode placement in the anode chamber for the (a) brush and (b) felt anodes. The felt anode becomes slightly bowed in shape due to a gasket holding it in place.

cathode and AEM, with the catalyst side of the cathode facing the membrane.

Headspace gas was collected through a glass tube glued to the top of the cathode chamber over a hole on the top of the chamber, with the top of the tube sealed with a butyl rubber stopper and aluminum crimp cap [34]. Gas was collected using a needle through the stopper that connected the tube to a 100 mL gas collection bag (Cali-5-Bond, Calibrated Instruments, NY).

Reactor operation

All anodes were acclimated using an inoculum from another well acclimated MFC, using a 1:1 mixture of MFC effluent and a sodium acetate (2 g/L) medium [50 mM phosphate buffer solution (PBS), containing (per liter of distilled water): 4.58 g Na_2HPO_4, 2.45 g NaH_2PO_4, 0.31 g NH_4Cl, 0.13 g KCl, and mineral and vitamin solutions [18]) until the MFCs reached a maximum voltage of 0.1 V, and then the MFCs were switched to only the acetate medium. The MFCs were operated in fed-batch mode in a 30 °C temperature controlled room, with triplicate reactors for each anode type, and a 1000 Ω resistor in the circuit. Once steady potentials were reached over several cycles, polarization tests were conducted, and then the anodes were moved into the MECs that were operated using 0.9 V applied using a power supply (BK Precision, USA). The MEC reactors were tested with the same 50 mM PBS medium as used in MFCs for the anolyte, with 50 mM PBS as the catholyte. The pH of both electrolytes was 7.1, with an anolyte conductivity of 8.1 mS/cm, and a catholyte conductivity of 6.7 mS/cm. Before each cycle the catholyte was sparged with high purity nitrogen gas (99.998%) for 10 min to remove oxygen.

Measurements and calculations

Polarization tests were conducted for the brush anode MFCs by using different resistances over a single fed-batch cycle (single-cycle polarization test). Polarization data for the felt anodes were obtained using a single resistance for a complete cycle, with different resistors over multiple cycles (multiple cycle test) [41,42]. A multiple cycle polarization test was used for the felt reactors to reduce the likelihood of power overshoot [42], as preliminary tests using the felt anodes and the single cycle method showed substantial power overshoot in the power density curves. Reference electrodes were used to measure the electrode potentials (Ag/AgCl; +0.209 V vs SHE, model RE-5B, BASi, IN). A single reference electrode was used in the brush MFC reactor to measure both the anode and cathode potentials. The electrode spacing was much greater in the felt anode MFC reactors, so a different reference electrode measured the electrode potentials; one for the anode and one for the cathode (Fig. S1b). The use of the two reference electrodes minimized the distance and solution resistance between the reference and measured electrode, resulting in more accurate electrode measurements.

Current generation of the MECs was collected every 20 min using a multimeter (Model 2700, Keithley Instruments, Inc., OH) by measuring the voltage drop across a 10 Ω resistor in the circuit. The average current density was calculated based on the current needed to recover 90% of the total charge over the fed batch cycle, normalized to the cathode surface area (I_{90}, A/m^2) [43]. This approach minimizes the impact of long tails with low current at the end of the cycle, on the calculation of an average current.

The gas in the gas bag and the cathode headspace were analyzed for hydrogen using a gas chromatograph (Model 8610B, SRI Instruments Inc., USA). Each time the gas was analyzed, the influent and effluent COD were monitored using standard methods (method 5220, HACH company, CO), and the pH and conductivity were measured using a probe and meter (Seven-Multi, Mettler-Toledo International Inc).

The measured volume of hydrogen (v_{H2}, m^3) was calculated using the gas bag method, based on injecting a small volume of nitrogen gas in the bag prior to measurements [44]. The hydrogen production rate (Q_{H2}, m^3-H_2/m^3-d) was calculated as:

$$Q_{H2} = \frac{V_{H2}}{v_r \Delta t} \quad (1)$$

where v_r is the total volume of the reactor (m^3), and Δt is the reaction time (d). The theoretical moles of hydrogen produced due to the current measured was calculated as:

$$n_{CE} = \frac{\int_0^T I\, dt}{2F} \quad (2)$$

where I is the current (A), F is Faraday's constant (96485 C/mole e^-), and T is the total time. The percent of hydrogen recovered from the current, called the cathodic hydrogen recovery, was calculated as $r_{cat} = n_{H2}/n_{CE}$, where n_{H2} is the amount of moles of hydrogen recovered from the catholyte [34]. Coulombic efficiency was calculated from n_{CE} as $CE = n_{CE}/n_{th}$, where n_{th} is the theoretical number of moles of hydrogen that can be produced from the change in COD [10]. COD

removal was calculated as $COD_{rem} = \Delta COD/COD_i$, where ΔCOD is the change in COD from the initial COD (COD_i) and the final COD [1]. The overall hydrogen recovered is the ratio of the hydrogen recovered to the theoretical recovery based on COD removal, or $r_{H2} = n_{H2}/n_{th}$. Energy recovery (η_E) was relative to the maximum theoretical energy recovery under standard conditions as:

$$\eta_E = \frac{1.23}{E_{ps}} r_{cat} \quad (3)$$

where 1.23 V is the theoretical amount of voltage needed to split water, and E_{ps} is the applied voltage (0.9 V) using the power source [1].

Results and discussion

Power comparison for felt vs. brush anodes in MFCs

Power densities produced by the felt anode MFCs were lower than those of the brush anode MFCs, which was expected due to the larger spacing between the felt anode and cathode, and previous analysis of the performance of these electrodes in MFCs [23]. The maximum power density using the felt anodes in MFCs was 0.80 ± 0.02 W/m^2, compared to 1.69 ± 0.10 W/m^2 for the brush anode MFCs (Fig. 2a). The cathode potentials were similar for all reactors based on the current, indicating the differences in power densities were due to the brush versus felt anode potentials (Fig. 2b). The larger electrode spacing distance between the felt anode and cathode (needed to avoid oxygen contamination of the anode) resulted in a much higher ohmic resistance between electrodes compared to the brush anodes. For example, at a current density of 3.4 A/m^2, 130 mV of potential is lost due to the solution conductivity (8.12 mS/cm) for an electrode spacing of 3.1 cm (from the felt surface to cathode distance), compared to only 13 mV for 0.3 cm between the outer brush surface to the cathode (using Ohm's Law, and solution resistance in the Supplemental Information, Eq. S(1)).

Current densities for felt vs. brush anodes in MECs

When the felt and brush anodes were transferred to the MECs, brush anodes still demonstrated better performance than the felt anodes based on average current densities and hydrogen production rates. The current profiles for the brush and felt anodes were noticeably different over a single fed batch cycle (Fig. 3). While the brush anode showed a plateau in current for about 40% of the total cycle time, the felt anode initially had a higher peak current, but it rapidly and steadily decreased throughout the rest of the cycle. Thus, the average current density for just the beginning of the fed batch cycle (100 min) with the felt anode MECs (7.7 A/m^2) was higher than that of the brush anode (5.9 A/m^2). However, when the analysis of current was evaluated for most of the ~24 h cycle, based on the I_{90} average current, the brush had a higher average current of $I_{90} = 4.2 \pm 0.5$ A/m^2, compared to the felt anode ($I_{90} = 3.4 \pm 0.1$ A/m^2) (Fig. 4). These differences in current demonstrated that the felt anode could perform as well as the brush anode at the beginning of the cycle in MECs, but that the brush anode

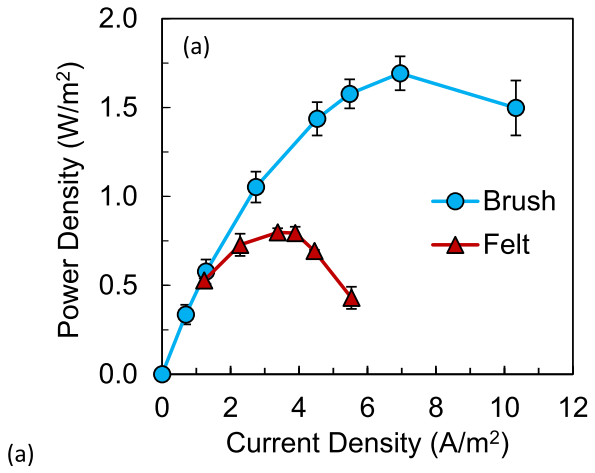

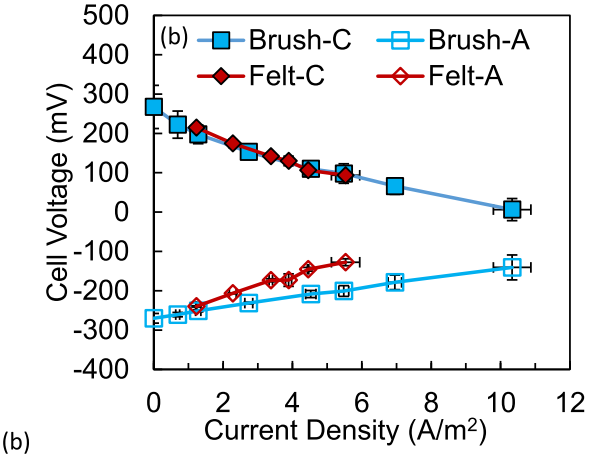

Fig. 2 – (a) MFC polarization tests using single-cycle (brush) and multi-cycle (felt) methods (b) Anode (A) and cathode (C) potentials.

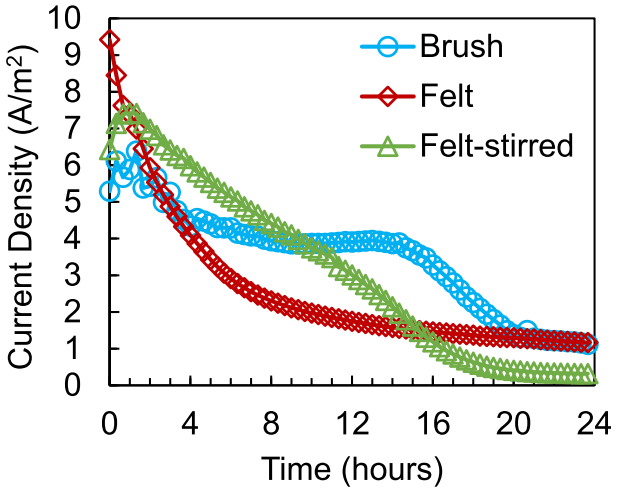

Fig. 3 – Example of average current density for one cycle of the MEC reactors for brush and felt anode MECs without stirring, and for felt anode MECs with stirring.

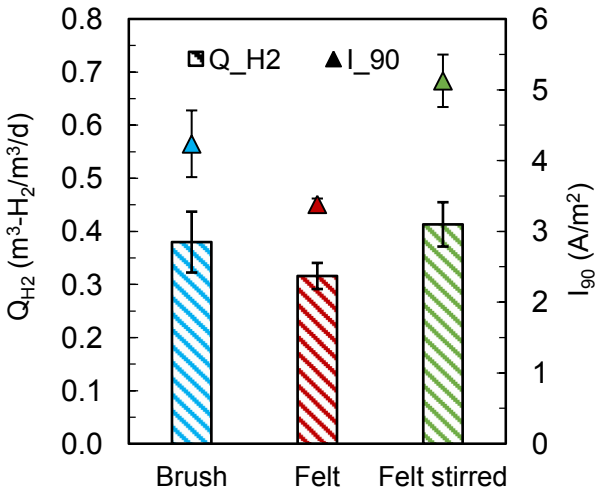

Fig. 4 – Average hydrogen production rates (Q_{H2}) and I_{90} current densities for brush and felt anode MECs without stirring, and for felt anode MECs with stirring.

produced better performance over the complete cycle. Since both felt and brush electrodes were placed close to the membrane, differences in performance were due to other factors than just electrode spacing.

Impact of stirring on current generation using felt anodes

The high peak and rapid decline in current over time for the felt anode MECs suggested that current generation was limited by substrate transport to the felt anode. Several factors could have contributed to substrate limited mass transfer to the felt anode: the denser structure of the felt anode compared to the more open brush anode structure; trapped water between the anode and AEM; and the small extension of the anode into the anode chamber compared to the brush which spanned nearly the complete width of the chamber (Fig. 1). Although the two types of anodes occupied the same volume of the anode chamber (4.4 mL for the brush, and 4.5 mL for the felt), the felt was more dense, as demonstrated by the effective volume of the anode chamber being 14 mL for the felt compared to 16 mL for the brush [45]. Trapped water between a membrane and an electrode can reduce performance as it can result in local pHs different from the bulk pH, and reduced ion transport [45].

The brush spanned nearly the full width of the chamber, and thus it was better immersed in the anolyte, which may have enabled better substrate transport to the bacteria on the brush fibers. In addition, a larger portion of the anolyte chamber was outside the electric field produced between the electrodes using the felt anode. Ion transport due to the electric field and molecular diffusion, in the absence of advective flow, can be described by the extended Nernst-Planck equation [46–48] as:

$$J_i = -D_i\nabla(c_i) - D_i\frac{z_iF}{RT}c_i\nabla(V) - D_ic_i\nabla(\ln\gamma_i) \quad (7)$$

where J is the chemical flux, i is the specific chemical species, c is the concentration, V is the potential, γ is the activity coefficient, T is the temperature, D is the diffusivity, R is the gas constant, and z is the charge of the species. For the felt anode, the electric field could not enhance the transport of negatively-charged acetate ions to the anode since most of the anolyte was in the space between the end plate and the felt surface. However, the brush anodes spanned nearly the complete width of the chamber, and thus a much greater proportion of the acetate was in the electric field between the two electrodes, and thus the electric field would favor transport of acetate ions to the anode. Simulations of the electric field in MFCs have shown that the electric field can enhance acetate ion transport to the brush surface [49], although biofilm models of ion transport suggest that the electric field contributes only 15% or less to power production in MFCs [47].

To test this hypothesis of substrate-limited mass transfer of acetate to the anode, the felt anolyte was stirred using a magnetic stir bar inserted into the anolyte chamber, to reduce concentration gradients near the anode. Stirring the felt anode anolyte clearly improved performance, likely by providing a higher average substrate concentration near the felt anode [47]. The average current over the cycle improved to $I_{90} = 5.1 \pm 0.4$ A/m^2, which was larger than that with the brush anode in the absence of stirring of $I_{90} = 4.2 \pm 0.5$ A/m^2 (Fig. 5). The anolyte in the MECs with brush anodes were not stirred due to the lack of space for the stir bar, but likely stirring the brush anolyte would also have increased the current densities of brush anodes. This result showing improved current production by stirring the felt anolyte, clearly demonstrated that performance of the anode was greatly impacted by substrate limited mass transfer in these MECs.

There were other factors that could have impacted current densities in these MECs. For example, localized pH changes can reduce current generation by an anode and cathode. The final pH of the anolytes, however, were similar with 6.2 ± 0.1 for the felt anode and 6.3 ± 0.0 for the brush anode. The final

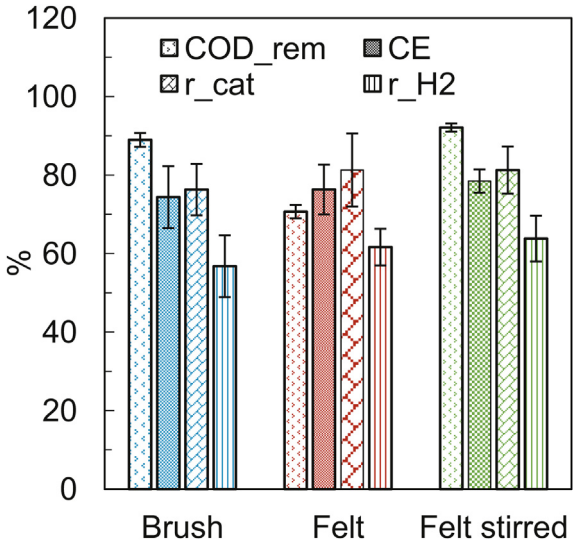

Fig. 5 – COD removal percentages (COD_{rem}), cathodic hydrogen recoveries (r_{cat}) and overall hydrogen recoveries (r_{H2}), and coulombic efficiencies (CE) for brush and felt anode MECs without stirring, and for felt anode MECs with stirring.

pH of the catholyte was higher for the brush anode MECs (8.7 ± 0.4) than the felt anode MECs (8.0 ± 0.2), due to the higher current densities and thus greater ion imbalances between the electrolyte chambers. A higher pH of the catholyte could reduce current generation, based on calculations of pH using the Nernst equation, but recent tests show that a higher catholyte pH can help to balance charge in the two chamber due to the increased concentration of hydroxide ions [50–54].

Impact of stirring on hydrogen production and other measures of performance

In general, brush anodes performed better than felt anodes without stirring, but felt anode performance was improved with stirring in many other aspects of MEC performance. The brush reactors had a higher hydrogen production rate of 0.38 ± 0.02 m^3-H_2/m^3-d averaged over the complete fed-batch cycle, compared to 0.32 ± 0.02 m^3-H_2/m^3-d for the felt anode MECs without stirring (Fig. 4). This higher hydrogen production rate for brush reactors was consistent with the higher average I_{90} current density. With stirring, the hydrogen production rate by the felt anodes increased to 0.41 ± 0.04 m^3-H_2/m^3-d.

COD removals were lower for the felt anode MECs compared to the brush anode MECs in the absence of stirring, consistent with the lower I_{90} current densities and hydrogen production rates (Fig. 5). Stirring increased COD removal by the felt anodes, from ΔCOD = 71 ± 2% (no stirring) to ΔCOD = 92 ± 1% (stirring).

Coulombic efficiencies were similar for all reactors, with CEs of 74 ± 8% using brushes, 76 ± 6% using felt anodes and 79 ± 3% with felt anodes and stirring (Fig. 5). The cathodic recoveries were slightly higher on average for the felt reactors than the brush reactors, resulting in slightly higher hydrogen recoveries for the felt reactors (r_{H2} = 62 ± 5% with no stirring, and 64 ± 6% with stirring) compared to the brush reactors (r_{H2} = 62 ± 5%). However, for all these values, the differences were small given the variability of the results based on standard deviations of about 10% of the averages. The energy recovery based on hydrogen production to only the electricity used (i.e., it does not include the energy in the acetate) was also larger for the felt reactors (111 ± 13%) with stirring than the brush reactors (104 ± 9%) without stirring, but both values were larger than 100% indicating more energy was recovered than what was being applied as electrical power. Coulombic efficiencies, and cathodic and hydrogen recoveries were not changed due to mixing of the anolyte with the felt anodes (Fig. 5).

Implications for using brush or felt anodes in MECs

Previous studies with MFCs with flat anodes have indicated that the main impact on power generation is oxygen contamination of the anode when it is placed too closely to the cathode [18,19]. However, for completely anaerobic MECs, oxygen contamination of the anode is not an issue. Even when the felt anodes were placed close to the cathode and against the AEM, brush anodes still performed better than the felt anodes in the absence of stirring. While the specific reason for the better performance of the brush anodes was not conclusively demonstrated here, it was shown that stirring significantly improved both current generation and hydrogen production rates of the felt anodes, demonstrating the importance of mass transfer limitations for the felt anodes. It is possible that the microbial communities on the anodes were not the same due to differences in the current densities and electrode potentials. It has been shown that electrode potentials influence the expression of different cytochromes by *Geobacter* species [55]. However, the largest changes in microbial communities occurs as a result of using different substrates [56]. When acetate is used as the fuel, the biofilms are always predominantly *Geobacter* [56–58]. It would be interesting, however, to see if the communities on the anodes changed over long term operation.

It is not clear whether these results here between brush and felt anodes in small reactors with fed-batch operation could be translated to larger-scale reactors with continuous flow, as the hydraulic and mass transfer conditions would be much different than those examined here. If a larger reactor was operated with continuous flow, it would likely not be practical to stir the liquid due to the energy requirements for mixing [20]. Also, the impact of flow over flat felt anodes, compared to flow over (or through) brush anodes cannot be predicted based on these experiments in the absence of such flow. Thus, the impact of flow past flat or brush anodes for continuous flow operations should be further examined relative to performance in both MECs and MFCs.

Conclusions

MECs with brush anodes had better hydrogen production rates than those with flat felt anodes in fed-batch tests, even when they were both placed close to the ion exchange membrane, in the absence of anolyte mixing. However, when the anolyte solution was mixed using a stir bar, the felt anode MECs (0.41 ± 0.04 m^3-H_2/m^3d) improved hydrogen production rates to levels slightly larger than brush anodes (no mixing). The improved performance of the felt anodes in MECs with stirring suggested that current generation was limited by substrate transport to the felt anodes. This substrate limited transport, and a lower current density without stirring, also reduced the extent of COD removal with felt anodes. However, with stirring and improved mass transfer of acetate to the anode biofilm, COD removal by the felt anodes was increased. As stirring is likely not practical for larger-scale MEC operation, as it increases the energy consumption, it is concluded that brush anodes would provide better performance than felt anodes for MECs.

Acknowledgments

The research was supported by funds provided by the National Renewable Energy Laboratory (NREL) through the Department of Energy (DOE) CPS Project #21263.

Appendix A. Supplementary data

Supplementary data related to this article can be found at https://doi.org/10.1016/j.ijhydene.2018.04.059.

REFERENCES

[1] Logan BE, Call D, Cheng S, Hamelers HVM, Sleutels THJA, Jeremiasse AW, et al. Microbial electrolysis cells for high yield hydrogen gas production from organic matter. Environ Sci Technol 2008;42:8630–40.

[2] Logan BE, Rabaey K. Conversion of wastes into bioelectricity and chemicals using microbial electrochemical technologies. Science 2012;337:686–90.

[3] Yu N, Xing D, Li W, Yang Y, Li Z, Li Y, et al. Electricity and methane production from soybean edible oil refinery wastewater using microbial electrochemical systems. Int J Hydrogen Energy 2017;42:96–102.

[4] Li F, Liu W, Sun Y, Ding W, Cheng S. Enhancing hydrogen production with Ni–P coated nickel foam as cathode catalyst in single chamber microbial electrolysis cells. Int J Hydrogen Energy 2017;42:3641–6.

[5] Wang L, Liu W, He Z, Guo Z, Zhou A, Wang A. Cathodic hydrogen recovery and methane conversion using Pt coating 3D nickel foam instead of Pt-carbon cloth in microbial electrolysis cells. Int J Hydrogen Energy 2017;42:19604–10.

[6] Kim K-Y, Zikmund E, Logan BE. Impact of catholyte recirculation on different 3-dimensional stainless steel cathodes in microbial electrolysis cells. Int J Hydrogen Energy 2017;42:29708–15.

[7] Hasany M, Mardanpour MM, Yaghmaei S. Biocatalysts in microbial electrolysis cells: a review. Int J Hydrogen Energy 2016;41:1477–93.

[8] Liu H, Grot S, Logan BE. Electrochemically assisted microbial production of hydrogen from acetate. Environ Sci Technol 2005;39:4317–20.

[9] Rozendal RA, Hamelers HVM, Euverink GJW, Metz SJ, Buisman CJN. Principle and perspectives of hydrogen production through biocatalyzed electrolysis. Int J Hydrogen Energy 2006;31:1632–40.

[10] Ivanov I, Ahn Y, Poirson T, Hickner MA, Logan BE. Comparison of cathode catalyst binders for the hydrogen evolution reaction in microbial electrolysis cells. Int J Hydrogen Energy 2017;42:15739–44.

[11] Cusick RD, Kim Y, Logan BE. Energy capture from thermolytic solutions in microbial reverse-electrodialysis cells. Science 2012;335:1474–7.

[12] Logan BE. Microbial fuel cells. Hoboken, NJ: John Wiley & Sons, Inc; 2008.

[13] Logan BE. Environmental transport processes. New York: Wiley; 1999.

[14] Logan BE. Essential data and techniques for conducting microbial fuel cell and other types of bioelectrochemical system experiments. ChemSusChem 2012;5:988–94.

[15] Logan BE, Wallack MJ, Kim K-Y, He W, Feng Y, Saikaly PE. Assessment of microbial fuel cell configurations and power densities. Environ Sci Technol Lett 2015;2:206–14.

[16] Fan Y, Hu H, Liu H. Enhanced coulombic efficiency and power density of air-cathode microbial fuel cells with an improved cell configuration. J Power Sources 2007;171:348–54.

[17] Fan Y, Sharbrough E, Liu H. Quantification of the internal resistance distribution of microbial fuel cells. Environ Sci Technol 2008;42:8101–7.

[18] Cheng S, Liu H, Logan BE. Increased power generation in a continuous flow MFC with advective flow through the porous anode and reduced electrode spacing. Environ Sci Technol 2006;40:2426–32.

[19] Hays S, Zhang F, Logan BE. Performance of two different types of anodes in membrane electrode assembly microbial fuel cells for power generation from domestic wastewater. J Power Sources 2011;196:8293–300.

[20] Hutchinson AJ, Tokash JC, Logan BE. Analysis of carbon fiber brush loading in anodes on startup and performance of microbial fuel cells. J Power Sources 2011;196:9213–9.

[21] Logan BE, Cheng S, Watson V, Estadt G. Graphite fiber brush anodes for increased power production in air-cathode microbial fuel cells. Environ Sci Technol 2007;41:3341–6.

[22] Yang W, Kim K-Y, Saikaly PE, Logan BE. The impact of new cathode materials relative to baseline performance of microbial fuel cells all with the same architecture and solution chemistry. Energy Env Sci 2017;10:1025–33.

[23] Ahn Y, Logan BE. Altering anode thickness to improve power production in microbial fuel cells with different electrode distances. Energ Fuel 2012;27:271–6.

[24] Gil-Carrera L, Mehta P, Escapa A, Morán A, García V, Guiot SR, et al. Optimizing the electrode size and arrangement in a microbial electrolysis cell. Bioresour Technol 2011;102:9593–8.

[25] Lanas V, Ahn Y, Logan BE. Effects of carbon brush anode size and loading on microbial fuel cell performance in batch and continuous mode. J Power Sources 2014;247:228–34.

[26] Oh S, Min B, Logan BE. Cathode performance as a factor in electricity generation in microbial fuel cells. Environ Sci Technol 2004;38:4900–4.

[27] Wei J, Liang P, Huang X. Recent progress in electrodes for microbial fuel cells. Bioresour Technol 2011;102:9335–44.

[28] Wu S, He W, Yang W, Ye Y, Huang X, Logan BE. Combined carbon mesh and small graphite fiber brush anodes to enhance and stabilize power generation in microbial fuel cells treating domestic wastewater. J Power Sources 2017;356:348–55.

[29] Kang H, Jeong J, Gupta PL, Jung SP. Effects of brush-anode configurations on performance and electrochemistry of microbial fuel cells. Int J Hydrogen Energy 2017;42:27693–700.

[30] Lee H-S, Torres CsI, Parameswaran P, Rittmann BE. Fate of H_2 in an upflow single-chamber microbial electrolysis cell using a metal-catalyst-free cathode. Environ Sci Technol 2009;43:7971–6.

[31] Call D, Merrill MD, Logan BE. High surface area stainless steel brushes as cathodes in microbial electrolysis cells (MECs). Environ Sci Technol 2009;43:2179–83.

[32] Call DF, Wagner RC, Logan BE. Hydrogen production by Geobacter species and a mixed consortium in a microbial electrolysis cell. Appl Environ Microbiol 2009;75:7579–87.

[33] Wang A, Liu W, Cheng S, Xing D, Zhou J, Logan BE. Source of methane and methods to control its formation in single chamber microbial electrolysis cells. Int J Hydrogen Energy 2009;34:3653–8.

[34] Call D, Logan BE. Hydrogen production in a single chamber microbial electrolysis cell (MEC) lacking a membrane. Environ Sci Technol 2008;42:3401–6.

[35] Escapa A, San-Martín MI, Mateos R, Morán A. Scaling-up of membraneless microbial electrolysis cells (MECs) for domestic wastewater treatment: bottlenecks and limitations. Bioresour Technol 2015;180:72–8.

[36] Feng Y, Yang Q, Wang X, Logan BE. Treatment of graphite fiber brush anodes for improving power generation in air-cathode microbial fuel cells. J Power Sources 2010;195:1841–4.

[37] Lanas V, Logan BE. Evaluation of multi-brush anode systems in microbial fuel cells. Bioresour Technol 2013;148:379–85.

[38] Zhang F, Cheng S, Pant D, Bogaert GV, Logan BE. Power generation using an activated carbon and metal mesh cathode in a microbial fuel cell. Electrochem Commun 2009;11:2177–9.

[39] Pant D, Bogaert GV, Smet MD, Diels L, Vanbroekhoven K. Use of novel permeable membrane and air cathodes in acetate microbial fuel cells. Electrochim Acta 2010;55:7710–6.

[40] Zhang F, Pant D, Logan BE. Long-term performance of activated carbon air cathodes with different diffusion layer porosities in microbial fuel cells. Biosens Bioelectron 2011;30:49–55.
[41] Velásquez-Orta SB, Curtis TP, Logan BE. Energy from algae using microbial fuel cells. Biotechnol Bioeng 2009;103:1068–76.
[42] Watson VJ, Logan BE. Analysis of polarization methods for elimination of power overshoot in microbial fuel cells. Electrochem Commun 2011;13:54–6.
[43] Ivanov I, Ren L, Siegert M, Logan BE. A quantitative method to evaluate microbial electrolysis cell effectiveness for energy recovery and wastewater treatment. Int J Hydrogen Energy 2013;38:13135–42.
[44] Ambler JR, Logan BE. Evaluation of stainless steel cathodes and a bicarbonate buffer for hydrogen production in microbial electrolysis cells using a new method for measuring gas production. Int J Hydrogen Energy 2011;36:160–6.
[45] Zhang X, Cheng S, Huang X, Logan BE. Improved performance of single-chamber microbial fuel cells through control of membrane deformation. Biosens Bioelectron 2010;25:1825–8.
[46] Marcus AK, Torres CI, Rittmann BE. Conduction-based modeling of the biofilm anode of a microbial fuel cell. Biotechnol Bioeng 2007;98:1171–82.
[47] Marcus AK, Torres CI, Rittmann BE. Evaluating the impacts of migration in the biofilm anode using the model PCBIOFILM. Electrochim Acta 2010;55:6964–72.
[48] Samson E, Marchand J. Numerical solution of the extended Nernst-Planck model. J Colloid Interface Sci 1999;215:1–8.
[49] Ahn Y, Hatzell MC, Zhang F, Logan BE. Different electrode configurations to optimize performance of multi-electrode microbial fuel cells for generating power or treating domestic wastewater. J Power Sources 2014;249:440–5.
[50] Popat SC, Ki D, Rittmann BE, Torres CI. Importance of OH^- transport from cathodes in microbial fuel cells. ChemSusChem 2012;5:1071–9.
[51] Ye Y, Zhu X, Logan BE. Effect of buffer charge on performance of air-cathodes used in microbial fuel cells. Electrochim Acta 2016;194:441–7.
[52] Ye Y, Logan BE. The importance of OH– transport through anion exchange membrane in microbial electrolysis cells. Int J Hydrogen Energy 2018;43:2645–53.
[53] Ruiz Y, Baeza JA, Guisasola A. Microbial electrolysis cell performance using non-buffered and low conductivity wastewaters. Chem Eng J 2016;289:341–8.
[54] Ruiz Y, Baeza JA, Guisasola A. Enhanced performance of bioelectrochemical hydrogen production using a pH control strategy. ChemSusChem 2015;8:389–97.
[55] Zhu X, Yates MD, Logan BE. Set potential regulation reveals additional oxidation peaks of *Geobacter sulfurreducens* anodic biofilms. Electrochem Commun 2012;22:116–9.
[56] Kiely PD, Regan JM, Logan BE. The electric picnic: synergistic requirements for exoelectrogenic microbial communities. Curr Biotechnol 2011;22:378–85.
[57] Yates MD, Kiely PD, Call DF, Rismani-Yazdi H, Bibby K, Peccia J, et al. Convergent development of anodic bacterial communities in microbial fuel cells. ISME J 2012;6:2002–13.
[58] Holmes DE, Bond DR, O'Neil RA, Reimers CE, Tender LR, Lovley DR. Microbial communities associated with electrodes harvesting electricity from a variety of aquatic sediments. Microb Ecol 2004;48:178–90.